

I am pleased to provide you complimentary one-time access to my article as a PDF file for your own personal use. Any further/multiple distribution, publication or commercial usage of this copyrighted material would require submission of a permission request to the publisher.

Timothy M. Miller, MD, PhD

ALS-linked mutant superoxide dismutase 1 (SOD1) alters mitochondrial protein composition and decreases protein import

Quan Li^{a,1}, Christine Vande Velde^{b,c,1}, Adrian Israelson^b, Jing Xie^d, Aaron O. Bailey^e, Meng-Qui Dong^e, Seung-Joo Chun^a, Tamal Roy^b, Leah Winer^a, John R. Yates^e, Roderick A. Capaldi^d, Don W. Cleveland^{b,2}, and Timothy M. Miller^{a,b,2}

^aDepartment of Neurology, Hope Center for Neurological Disorders, The Washington University School of Medicine, St. Louis, MO 63110; ^bLudwig Institute and Departments of Cellular and Molecular Medicine and Neuroscience, University of California at San Diego, La Jolla, CA 92093-0670; ^cDepartment of Medicine, Centre Hospitalier de l'Université de Montréal Research Center, Université de Montréal, Montreal, QC, Canada H2L 4M1; ^dDepartment of Cell Biology, The Scripps Research Institute, La Jolla, CA 92037; and ^eMitoSciences, Eugene, OR 97403

Contributed by Don W. Cleveland, October 18, 2010 (sent for review February 4, 2010)

Mutations in superoxide dismutase 1 (SOD1) cause familial ALS. Mutant SOD1 preferentially associates with the cytoplasmic face of mitochondria from spinal cords of rats and mice expressing SOD1 mutations. Two-dimensional gels and multidimensional liquid chromatography, in combination with tandem mass spectrometry, revealed 33 proteins that were increased and 21 proteins that were decreased in SOD1^{G93A} rat spinal cord mitochondria compared with SOD1^{WT} spinal cord mitochondria. Analysis of this group of proteins revealed a higher-than-expected proportion involved in complex I and protein import pathways. Direct import assays revealed a 30% decrease in protein import only in spinal cord mitochondria, despite an increase in the mitochondrial import components TOM20, TOM22, and TOM40. Recombinant SOD1^{G93A} or SOD1^{G85R}, but not SOD1^{WT} or a Parkinson's disease-causing, misfolded α -synuclein^{E46K} mutant, decreased protein import by >50% in nontransgenic mitochondria from spinal cord, but not from liver. Thus, altered mitochondrial protein content accompanied by selective decreases in protein import into spinal cord mitochondria comprises part of the mitochondrial damage arising from mutant SOD1.

motor neuron disease | proteomic | neurodegenerative disease | amyotrophic

Amyotrophic lateral sclerosis (ALS) is an adult-onset neurodegenerative disorder caused by loss of the motor neurons within the spinal cord and dysfunction of the motor pathways in the cortex (1, 2). Most cases of ALS (90%) are sporadic. Of the 10% of cases that are inherited, about one-fifth are caused by mutation within the superoxide dismutase 1 (SOD1) gene. Rodents expressing mutant SOD1 develop an ALS-like disease (1, 2). A consensus has emerged that disease arises from acquisition by the mutant proteins of one or more toxic properties, rather than from loss of dismutase activity (3, 4). At least eight prominent mutant-derived toxicities have been proposed, including mitochondrial dysfunction, excitotoxicity, endoplasmic reticulum stress, toxic extracellular SOD1, superoxide production from microglia or astrocytes, and disruption of the blood-brain barrier (5). Furthermore, pathogenesis is noncell autonomous with disease progression driven by mutant synthesis in astrocytes (6–8) and microglia (3, 9).

Dysfunction of mitochondria can clearly cause specific damage to neurons or muscle because deletion/mutation in mitochondrial genes causes specific nerve and muscle diseases (10). Accompanying mutant SOD1-mediated disease in some mice is evidence for altered mitochondrial calcium-buffering capacity (11) and changes in the activity of complexes of the electron transport chain (12). Deletion of the mitochondrial BCL-2-related proteins BAX and BAK delays disease onset in SOD1^{G93A} mice (13), perhaps by modulating effects of SOD1 conformational changes to BCL-2 (14). Apparent damage to mitochondria has been reported in autopsy material from ALS patients (15, 16).

Although SOD1 is a primarily cytosolic enzyme, wild-type SOD1 is also found in the intermembrane space of mitochondria in liver (17) and in yeast (18, 19). However, in the normal nervous

system very little SOD1 is found in or on mitochondria (20, 21), but mutant SOD1 has been found associated presymptomatically with the cytoplasmic face of mitochondria from spinal cord in all rodent models of SOD1 mutant-mediated disease (20, 21). A criticism that apparent association of dismutase inactive mutants with mitochondria might reflect cosedimentation of protein aggregates rather than bona fide mitochondrial association (22) has been refuted by demonstrating that mutant SOD1 floats with mitochondria rather than sedimenting as much more dense protein-only aggregates would under such conditions (21). Indeed, a portion of misfolded mutant SOD1 directly binds to the cytoplasmic facing surface of the major voltage-dependent anion channel (VDAC1), a general diffusion pore for anions and cations that is located on the outer mitochondrial membrane. Mutant SOD1 binding reduces conductance by purified VDAC1 reconstituted in a lipid bilayer, and spinal cord mitochondria have reduced ADP uptake (23).

Three prior efforts have reported use of proteomic tools to investigate how mutant SOD1 affects mitochondrial protein composition within whole-spinal-cord extracts of dismutase-active (24) or dismutase-inactive (25) SOD1 mutant mouse models or, more selectively, within mitochondria of a cell line retaining some motor neuron-like properties and expressing one dismutase-active, ALS-linked SOD1 mutant (26). We extended these approaches to determine whether mutant SOD1 affects protein content of spinal cord mitochondria before disease initiation in rodent models that develop ALS-like disease. Using a combination of mass spectrometry and 2D gels, we now report 21 proteins to be decreased approximately twofold, with another 33 that are increased by a comparable amount or more in mitochondria isolated from spinal cords of mutant SOD1 animals, accompanied by diminished protein import activity. By using purified components, inhibition of mitochondrial protein import is demonstrated to be a direct result of mutant but not wild-type SOD1.

Results

Altered Spinal Cord Mitochondrial Protein Content in SOD1 Mutant Rats. To identify possible differences in protein composition between mitochondria isolated from spinal cords of age-matched SOD1^{WT} and SOD1^{G93A} mutant rats, we used 2D gel electrophoresis as well as liquid chromatography followed by tandem mass spectrometry [multidimensional protein identification tech-

Author contributions: Q.L., C.V.V., R.A.C., D.W.C., and T.M.M. designed research; Q.L., C.V.V., A.I., J.X., A.O.B., M.-Q.D., S.-J.C., T.R., L.W., and T.M.M. performed research; Q.L., C.V.V., A.I., J.X., A.O.B., M.-Q.D., S.-J.C., T.R., L.W., J.R.Y., R.A.C., D.W.C., and T.M.M. analyzed data; and Q.L., C.V.V., D.W.C., and T.M.M. wrote the paper.

The authors declare no conflict of interest.

¹Q.L. and C.V.V. contributed equally to this work.

²To whom correspondence may be addressed. E-mail: millert@neuro.wustl.edu or dcleveland@ucsd.edu.

This article contains supporting information online at www.pnas.org/lookup/suppl/doi:10.1073/pnas.1014862107/-DCSupplemental.

nology (MudPIT)] (27). Initially, a presymptomatic age (11 wk) was chosen because it was known to correspond to a time of very active denervation of lower motor neurons (28). Although a change in staining on 2D gels may reflect altered abundance, size, or isoelectric point, the overall patterns of major proteins (visible in Coomassie (Fig. 1) or silver (Fig. S1) staining were highly similar. Twelve spots (Fig. 1 *B* and *C* compared with Fig. 1 *E* and *F* and Fig. S1 *B* and *C* compared with Fig. S1 *E* and *F*) were clearly different between the two samples, with five (spots 1, 6, 7, 8, and 9) increased in SOD1^{G93A} mitochondria and seven (spots 2–5 and 10–12) decreased. Each was excised, digested with trypsin, and identified via tandem mass spectrometry (Table S1). Three spots contained more than one protein, resulting in a total of 15 proteins identified.

Using MudPIT mass spectrometry, protein differences were also identified from three independent preparations of mitochondria from 11-wk-old SOD1^{WT} and age-matched presymptomatic SOD1^{G93A} rat spinal cords, using normalized spectral counts as an indication of the relative amount of any given protein (29, 30). We identified 299 mitochondrial proteins present in all of the mitochondrial samples. Most proteins (259) were unchanged in apparent abundance. However, 12 proteins were decreased by >0.6-fold and 28 proteins were increased by >1.8-fold (Table 1 and Table S2).

Hsp10, a cofactor for mitochondrial Hsp60 (31) and known to work as a stoichiometric partner chaperone for intramitochondrial protein folding, was predicted to be increased by mass spectrometry of SOD1^{G93A} mitochondria (Table 1). Immunoblotting of whole-spinal-cord mitochondrial extract from rat SOD1^{G93A} confirmed induction (1.4-fold, $P < 0.05$) of Hsp10, but not of Hsp60, in SOD1^{G93A} mitochondria versus SOD1^{WT} mitochondria. Similar immunoblotting of mitochondria from human spinal cords of patients with SOD1^{A4V} or SOD1^{I113T} mutations revealed even more substantial increases (4.5- and 2.5-fold, respectively), in Hsp10 (Fig. 2).

Decreased VDAC and cytochrome *c* oxidase subunits and increased adenylate kinase 2 seen here mirrored changes in whole-spinal-cord extracts from a mutant SOD1 mouse (24). Decreased VDAC, aconitase, isocitrate dehydrogenase (IDH3), and ATP synthase subunits and increased NDUFB8, a component of the electron transport complex I (see below), were found, similar to changes seen in mitochondria from an ALS-linked SOD1 mutant expressing a motor neuron-like cell line (26). 4-Aminobutyrate aminotransferase was increased and IDH3 was decreased in SOD1^{G93A} mitochondria, as assessed here by both 2D gels and mass spectrometry.

Only 26 mitochondrial proteins showed greater than twofold changes increased in SOD1^{G93A} spinal cord mitochondria relative to mitochondria from age-matched SOD1^{WT} rats expressing wild-type human SOD1 at comparable levels. Three of these are involved in protein import into mitochondria (TOM40, TOM20, and TOM22).

Decreased Complex I Activity in Mitochondria from SOD1^{G93A} Rats. Six (NDUFS1, ND5, NDUFB8, NDUFC2, NDUFA5, NDUFB9) of the 26 down-regulated proteins in mitochondria from mutant spinal cord are components of the 42-subunit complex I, also known as NADH dehydrogenase. Complex I is located on the inner membrane of mitochondria, catalyzes the shuttling of electrons from NADH to coenzyme Q, and helps to build the proton gradient required for ATP generation. Immunoprecipitation of mitochondrial extracts with a monoclonal antibody raised against complex I, which had been crosslinked to protein G agarose beads (32), confirmed that at least six complex I polypeptides were changed in relative abundance: two were increased [(V1, S2) and (A10, ND5)] and four were decreased [S1, (A9, D1), S3, and (B10, V2; B7, A5, B4, B5, B6, S5, B16, 6, A7)] (some stained bands represent multiple polypeptides) (Fig. 3A). Of those decreased in SOD1^{G93A} mitochondria, a polypeptide migrating at 75 kDa (Fig. 3A) most likely represents S1 (also known as NDUFS1) (32–34), which was also seen to be decreased by mass spectrometry (Table 1) and 2D gels (Fig. 3B, arrows). A prominent complex I polypeptide migrating at 35 kDa, most likely representing ND5 (32–34), was increased in immunoprecipitates. ND5 is a mitochondrially encoded core subunit of complex I believed to be important for catalysis (33). Mass spectrometry confirmed the identity of ND5 and its increased relative abundance (Table 1). Protein changes were more prominent in the spinal cord than in the liver (Fig. 3A).

Complex I activity, measured by first immunoprecipitating the enzyme complex and subsequently measuring the passage of electrons to the colorimetric electron acceptor dye NBT (34), was 50% higher in liver versus spinal mitochondrial samples (normalized to citrate synthase activity). Activity was decreased by 25% in SOD1^{G93A} spinal cord mitochondria from symptomatic animals relative to mitochondria from SOD1^{WT} animals (Fig. 3C). Surprisingly, a comparable decrease (30%) was also seen in complex I immunoprecipitated from mitochondria purified from livers of the same animals.

Protein Import Is Slowed in SOD1^{G93A} Spinal Cord Mitochondria.

Immunoblotting of extracts from isolated spinal cord mitochondria was used to more directly test the apparent increases in proteins involved in mitochondrial protein import that were found by mass spectrometry. For TOM40, a twofold increase was readily apparent in comparing its accumulated level (relative to COX4; Fig. 4A, *Bottom*) in SOD1^{WT} and SOD1^{G93A} mitochondrial extracts. A similar increase in full-length TOM40 was seen in liver mitochondria from mutant animals. In addition, an immunoreactive polypeptide of increased mobility (corresponding to ~37 kDa) was found in the liver, but not in spinal cord fractions; this polypeptide too was elevated in mutant mitochondria. mRNA encoding TOM20, TOM22, and TOM40 were not significantly different in liver or spinal cord between SOD1^{WT} versus SOD1^{G93A} rats (Fig. S2). Isolated mitochondria from human lumbar spinal cord from a SOD1^{A4V} patient and SOD1^{I113T} patient showed a similar increase in TOM40 compared with control (Fig. 4B). Although parallel analyses for TOM20 and TOM22

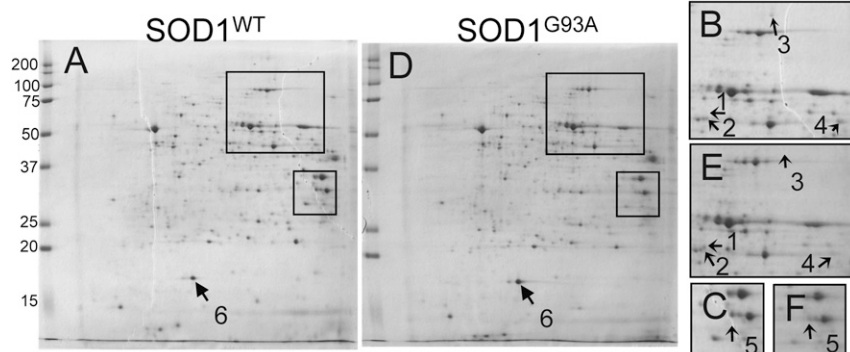


Fig. 1. Two-dimensional gel analysis of mitochondrial from SOD1 rats. Mitochondria were isolated from asymptomatic (*A*, *B*, *C*) SOD1^{WT} and (*D*, *E*, *F*) SOD1^{G93A} rats, separated by 2D gel electrophoresis, and stained with Coomassie blue. Spots that were different between SOD1^{WT} and SOD1^{G93A} were excised, digested with trypsin, and analyzed by mass spectrometry. See Table S1 for protein determinations.

Table 1. Solution mass spectrometry analysis of mitochondria from SOD1^{WT} versus SOD1^{G93A} rats

Protein	Name	G93A/WT
SLC25A4	ADP/ATP translocase 1	0.4
ETFDH	Electron transfer flavoprotein-dehydrogenase	0.5
NDUF51	NADH-ubiquinone oxidoreductase 75-kDa subunit, mitochondrial precursor	0.5
PHB	Prohibitin	0.5
MDH2	Malate dehydrogenase, mitochondrial precursor	0.5
COX5B	Cytochrome c oxidase subunit 5B, mitochondrial precursor	0.5
SLC25A5	ADP/ATP translocase 2	0.6
HSPD1	60-kDa heat-shock protein, mitochondrial precursor	0.6
ES1	ES1 protein homolog, mitochondrial precursor	0.6
AK2	Adenylate kinase 2	0.6
HADH	Hydroxyacyl-CoA dehydrogenase, mitochondrial precursor	0.6
COX6C2	Cytochrome c oxidase polypeptide Vic-2	0.6
HIBCH	3-hydroxyisobutyryl-Coa hydrolase, mitochondrial precursor	1.8
TOMM40	Probable mitochondrial import receptor subunit TOM40 homolog	1.8
DECR1	2,4 dienoyl-CoA reductase, mitochondrial precursor	1.8
MFN2	Mitofusin 2	1.8
DHTKD1	Dehydrogenase E1 and transketolase domain containing 1	1.9
ABAT	4-Aminobutyrate aminotransferase, mitochondrial precursor	1.9
AIFM1	Apoptosis-inducing factor 1, mitochondrial precursor	1.9
IDH2	Isocitrate dehydrogenase (NADP), mitochondrial precursor	1.9
Mut	Similar to methylmalonyl-CoA mutase, mitochondrial precursor	2
DBT	Dihydroliipoamide branched-chain transacylase E2	2
ND5	NADH dehydrogenase subunit 5	2.1
PYGB	Glycogen phosphorylase, brain form	2.2
NDUFB8	NADH dehydrogenase (ubiquinone) 1 β -subcomplex 8	2.3
ZADH2	Zinc-binding alcohol dehydrogenase, domain containing 2	2.3
IDH3B	Isocitrate dehydrogenase (NAD) subunit β , mitochondrial precursor	2.3
PCCA	Propionyl-CoA carboxylase α -chain, mitochondrial precursor	2.4
SOD2	Superoxide dismutase 2, mitochondrial precursor	2.4
TOMM22	TOM22	2.4
GDAP111	Ganglioside-induced differentiation-associated protein 1	2.5
NDUFC2	Hypothetical protein Ndufc2	2.5
ATPIF1	APTase inhibitor, mitochondrial precursor	2.5
NDUFA5	NADH dehydrogenase 1 α -subcomplex subunit 5	2.8
ABHD10	Abhydrolase domain-containing protein 10, mitochondrial precursor	3.1
TOMM20	Mitochondrial import receptor subunit TOM 20 homolog	3.6
NDUFB9	NADH dehydrogenase 1 β -subcomplex	3.8
COX6A1	Cytochrome c oxidase polypeptide Via-liver, mitochondrial precursor	5.9
SSBP1	Single-stranded DNA-binding protein, mitochondrial precursor	8
HSPE1	10-kDa heat-shock protein, mitochondrial Hsp 10	8

Mitochondrial proteins in SOD1^{WT} and SOD1^{G93A} spinal cord were identified by using solution mass spectrometry (MudPIT). Relative amount of proteins was calculated by spectral counts, and the ratios of SOD1^{G93A}:SOD1^{WT} were averaged from three independent results.

revealed only marginal increases for each in rat SOD1^{G93A} spinal cord, increases in both were clearly evident in human spinal cord mitochondria from both SOD1 mutant samples (Fig. 4*A* and *B*).

Because prior efforts had revealed a proportion of mutant SOD1 to be bound on the cytoplasmic face of mitochondria (21) and the changes documented above in TOM40, we tested whether protein import was altered in spinal mitochondria from SOD1^{G93A} or SOD1^{WT} rats. Ornithine transcarbamylase (OTC) was used as an initial mitochondrial import substrate. The 39-kDa initial translation product of OTC carries a well-characterized mitochondrial import sequence, which includes an amino terminal signal sequence that is cleaved following mitochondrial entry into the matrix (35). Successful OTC import can thus be detected by the appearance of the mature 36-kDa OTC polypeptide. ³⁵S-labeled OTC was synthesized *in vitro* and incubated with purified mitochondria and untransported OTC degraded by the addition of proteinase K. Within 15 min of incubation, the majority of OTC was successfully imported into mitochondria from liver or spinal cord of SOD1^{WT} rats (Fig. 4*C*). Parallel incubations with mitochondria from spinal cord of symptomatic SOD1^{G93A} rats revealed

a trend toward decrease (by ~15%) in import ability (from three independent preparations with triplicate measurements for each independent preparation).

To test import of a second substrate (whose ultimate destination is to a second compartment within mitochondria), we tested ³⁵S-labeled iron sulfur protein (ISP), whose import is mediated via a well-defined import sequence that targets ISP to the inner mitochondrial membrane (36). Spinal cord mitochondria from SOD1^{G93A} animals showed a significant 30% decrement ($P < 0.05$, Fig. 4*D*) in their import ability. In a similar comparison of import, liver mitochondria were unchanged for ISP import and only marginally decreased (~10%) for OTC (Fig. 4*C* and *D*).

Diminished Import of Spinal Cord Mitochondria Is Not Secondary to Decreased Membrane Potential, Complex IV Activity, or ATP Levels.

Because depletion of the mitochondrial transmembrane potential is a well-accepted inhibitor of mitochondrial protein import (37), we measured the transmembrane potential of isolated mitochondria using flow cytometry with the potentiometric dye TMRM. Depolarization of the mitochondrial membrane was easily

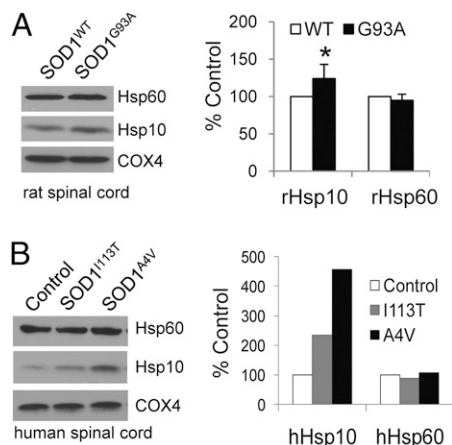


Fig. 2. Hsp10 is increased in rat and human ALS spinal cord mitochondria. Mitochondria were isolated (A) from SOD1^{WT} and SOD1^{G93A} rats, a nondiseased control patient, or (B) symptomatic ALS patients with SOD1^{A4V} or SOD1^{I113T} mutations. Proteins were separated by gel electrophoresis followed by immunoblotting for COX4, Hsp10, and Hsp60. Average \pm SD, $n = 4$, $*P < 0.05$.

detected after addition of CCCP or ADP, which, as expected, produced severe or partial depolarization, respectively (Fig. 5A). Membrane potential was not changed in SOD1^{G93A} symptomatic mitochondria compared with SOD1^{WT} (Fig. 5B).

Reduction in complex IV, the last enzyme of the electron transport chain that transfers electrons from cytochrome C to molecular oxygen and in the process pumps protons across the inner membrane, has been previously implicated by one prior study of mitochondria from SOD1^{G93A} mice (38). Although inhibition of this complex could secondarily affect protein import, no significant differences were detected between SOD1^{WT} and

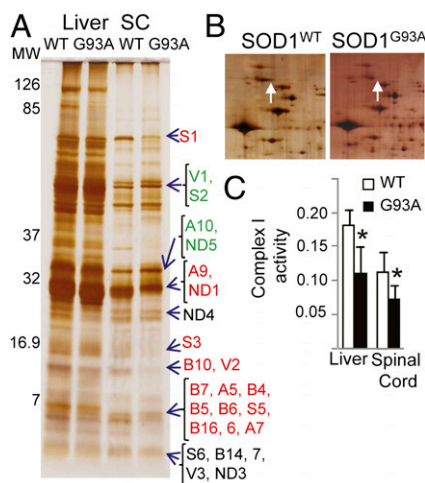


Fig. 3. SOD1^{G93A} causes changes in complex I protein composition and decreased complex I activity. (A) Mitochondria were isolated from symptomatic SOD1^{WT} and SOD1^{G93A} liver and spinal cord, and complex I was immunoprecipitated with an antibody that recognizes and immunoprecipitates the entire complex. Individual proteins were visualized by SDS/PAGE followed by silver staining. Labels for polypeptides that increased or decreased in the SOD1^{G93A} mitochondrial samples are green or red, respectively. Individual proteins are labeled here on the basis of the previous silver-staining analyses of isolated complex I. (B) Mitochondrial proteins from SOD1^{WT} and SOD1^{G93A} spinal cord were separated by 2D gels. The spot visually decreased in the SOD1^{G93A} sample (indicated by the arrow) was identified by mass spectrometry as S1 (also known as NDUFS1). (C) Complex I was immunoprecipitated from SOD1^{WT} and SOD1^{G93A} mitochondria, and the activity was determined and normalized to citrate synthase activity. Average \pm SD, $n = 4$, $*P < 0.05$.

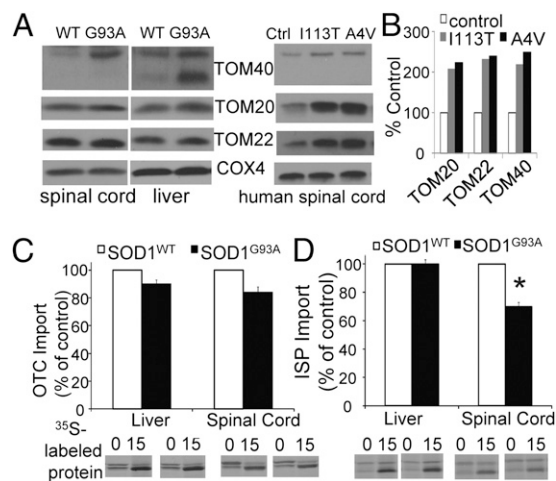


Fig. 4. TOM40 is increased and protein import is slowed in mitochondria from SOD1^{G93A}-expressing rats. (A) Mitochondria were isolated from SOD1^{WT} and SOD1^{G93A} rats, a nondiseased control patient, or (B) symptomatic ALS patients with SOD1^{A4V} or SOD1^{I113T} mutations. Proteins were separated by SDS/PAGE followed by immunoblotting for TOM20, TOM22, and TOM40. (C and D) Isolated mitochondria from symptomatic SOD1^{WT} or SOD1^{G93A} rats were incubated at 30 °C for 15 min with ³⁵S-labeled OTC or ³⁵S-labeled ISP. Proteins were separated by SDS/PAGE. The gel was dried and exposed for radioisotopic imaging. Graphs represent the percentage of import. Average \pm SD, $n = 4$, $*P < 0.05$. Representative gels are shown.

SOD1^{G93A} complex IV activities, despite a trend toward lower activity (Fig. S3A). Finally, although a deficit in protein import could also be secondary to overall ATP synthesis rates, ATP synthesis did not differ between symptomatic SOD1^{WT} and SOD1^{G93A} animals (Fig. S3B).

Direct Inhibition of Mitochondrial Protein Import by Mutant SOD1. To test for direct effects of mutant SOD1 on protein import, we combined mitochondria from spinal cord or liver of healthy nontransgenic rats with recombinant SOD1 proteins and then performed mitochondrial import assays. SOD1^{WT} protein had no effect on protein import of either of these isolated mitochondria preparations. In contrast, both SOD1^{G93A} and SOD1^{G85R} markedly decreased protein import of OTC (>50%) and ISP (>80%) ³⁵S-labeled proteins (Fig. 6) into spinal cord-derived mitochondria, but not of those isolated from liver. As with the mitochondria from SOD1^{G93A} rats (Fig. 4), the effect on ISP import was more

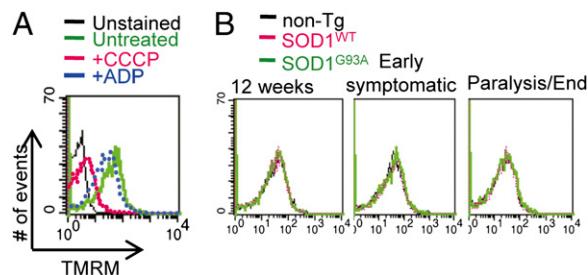


Fig. 5. Transmembrane potential is not changed in SOD1^{G93A} rats. (A and B) Mitochondria were isolated from nontransgenic, SOD1^{WT}, and SOD1^{G93A} transgenic rats. Mitochondria were stained with tetramethylrhodamine methyl ester (TMRM), a potentiometric dye that partitions into mitochondria on the basis of membrane potential. (A) TMRM staining shifts the signal two orders of magnitude. Depolarization of the membrane potential with CCCP or ADP decreases the TMRM signal and demonstrates the sensitivity of the assay. (B) There is no difference in membrane potential between SOD1^{G93A} rats that develop paralysis and nontransgenic or SOD1^{WT}-expressing animals. A representative of three independent experiments is presented.

pronounced. None of the recombinant SOD1 proteins affected transmembrane potential (Fig. S4). In addition, the absence of the effect of mutant SOD1 on protein import into liver mitochondria eliminated the possibility that the import deficit observed in spinal cord mitochondria derived from a mutant SOD1-mediated interference with the ^{35}S -labeled import substrates or other components of the assay. Mutations in α -synuclein cause Parkinson's disease and produce an encoded protein that misfolds (39, 40) and is linked to mitochondrial dysfunction (41). Unlike mutant SOD1, neither purified mutant (E46K) nor wild-type α -synuclein affected protein import into spinal cord mitochondria, even when added to 20 times higher levels than those at which import was impaired by SOD1 mutants (Fig. 6C).

Direct-binding targets of mutant SOD1 on the mitochondrial cytoplasmic face include VDAC1, which coimmunoprecipitates with mutant SOD1 whose binding to VDAC1 inhibits its conductance of adenine nucleotides (23). We determined that other direct-binding targets on the mitochondrial outer surface do exist because mutant SOD1 still binds to spinal cord-derived mitochondria from VDAC1 null mice (Fig. S5). Using immunoprecipitation for SOD1, we tested for direct binding of mutant SOD1 to the mitochondrial import components TOM20 and TOM40. Repeated attempts failed to generate evidence for an interaction, although antibody-binding sites could be occluded in any putative complex and transient interactions (as would be anticipated if mutant SOD1 were recognized as an import substrate) would not be expected to be detected by this kind of approach.

Discussion

Comparison of mitochondria from spinal cords of SOD1^{WT} versus SOD1^{G93A} rats revealed a handful of proteins whose abundance was substantially altered, accompanied by decreased protein import into spinal cord mitochondria from symptomatic SOD1^{G93A} animals. Elevation of the mitochondrial chaperone Hsp10 seen initially in mitochondria from SOD1 mutant rats was

even more prominently found in spinal mitochondria from human patients with either of two SOD1 mutations (Fig. 2). This is strongly indicative of the presence of an intramitochondrial stress that induces substantial elevation in this mitochondrial chaperone. Increased Hsp10, but not Hsp60, seen here in human mitochondria from SOD1 patients, is reminiscent of a similar divergence reported in subtypes of normal bone marrow cells (42) and in prostate cancer (43). In all, these findings raise the possibility of another function for Hsp10 within mitochondria in addition to its role as an obligate cofactor for Hsp60.

Complex I proteins were also affected, accompanied by diminished complex I activity in SOD1^{G93A} mitochondria, whereas complex IV activity, the mitochondrial membrane potential, and ATP synthesis rates were unaffected. Along with other reports of diminished respiratory chain activities in SOD1 mice (44), our evidence establishes deficits in complex I in liver mitochondria as well as in spinal cord mitochondria. Chronic inhibition of complex I is known to cause an increase in reactive oxygen species (45), which may, in turn, further damage mitochondria.

Overall, these data (i) demonstrate that mitochondria are indeed a target of mutant SOD1 toxicity and (ii) identify specific mitochondrial pathways that are damaged, including reduced protein import, induction of protein-folding chaperone capacity, and decreased complex I activity. Recognizing that there may be a bias toward recovery of healthy mitochondria in biochemical purifications (because more highly damaged mitochondria may be rapidly eliminated *in vivo* and/or preferentially lost in the differential centrifugation steps used for mitochondrial isolation), it is likely that these changes represent at least some of the initial changes in mitochondrial composition from mutant SOD1. A plausible view is that vulnerable spinal cord cells have a lower intrinsic threshold for accumulation of mitochondrial defects secondary to damage to direct targets of mutant SOD1, including chronic, partial inhibition of complex I. This would be consistent with previously documented differences in mitochondria derived from brain and other tissues following inhibition of respiratory complexes (46). Selective vulnerability may be derived from the known differences in protein composition in mitochondria from different tissues (30, 47), the cellular environment of various tissues, or other unknown factors.

Protein import represents a critical pathway for mitochondria because, among the ~1,400 estimated proteins in mitochondria, a mere 13 are encoded by mitochondrial DNA (47–49). The other ~1,387 proteins are delivered to mitochondria through the import pathways that we have demonstrated to be altered by SOD1 mutants, including changes in TOM40, TOM20, and TOM22. The increase in TOM20, TOM22, and TOM40 that we have found at the protein level occurred in mitochondria that were deficient in protein import. From this, we propose that the increased level of TOM components may reflect a response to a perceived deficit, although this response does not appear to be at the mRNA level because differences in TOM20, TOM22, and TOM40 mRNA were not found (Fig. S2). (Although increases in TOM proteins could reflect altered stoichiometry of import proteins that may itself lead to decreased import, the finding that liver mitochondria show increased TOM proteins, yet no deficit in import, argues against this proposal.)

Our evidence that mitochondria from SOD1^{G93A} rats do not import mitochondrial proteins as well as SOD1^{WT} rat mitochondria extends to ALS previous findings that deficits in mitochondrial protein import are linked to neurodegenerative diseases. Included here are mutations in TIM8a, a translocase of the mitochondrial inner membrane, which are causative for deafness and dystonia in Mohr-Tranebjerg syndrome (50). Furthermore, single nucleotide polymorphisms in the TOM40 gene have been associated with an increased risk for late-onset Alzheimer's disease (51, 52), and one previous study has suggested that amyloid- β associates directly with TOM40 (53). Thus, our data add to a growing body of evidence that deficits in mitochondrial protein import pathways may contribute to neurodegenerative diseases. A key next test to establish the importance of reduced mitochondrial

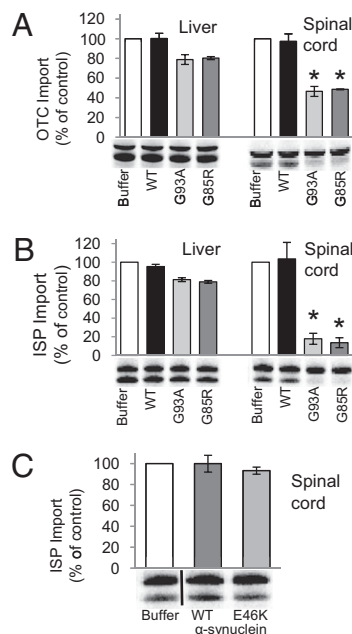


Fig. 6. Recombinant mutant SOD1 decreases spinal cord mitochondrial protein import. Mitochondria were isolated from nontransgenic rat liver or spinal cord and combined with 0.375 μM recombinant SOD1^{WT}, SOD1^{G93A}, and SOD1^{G85R} (A and B) or with 7.5 μM α -synuclein^{WT} or α -synuclein^{E46K} (C) proteins for 15 min at 30 °C. Then ^{35}S -labeled OTC (A) or ^{35}S -labeled ISP (B and C) was added for 15 min at 30 °C to the mitochondria to assess protein import. Proteins were separated by SDS/PAGE. The gel was dried and exposed for radioisotopic imaging. Graphs represent the percentage of import. Average \pm SD, $n = 3$, * $P < 0.05$. Representative gels are shown.

import in ALS pathogenesis will be to use gene-targeted mice to further alter import activity and assess how this affects disease.

Materials and Methods

Fresh mitochondria were isolated from rat liver and spinal cord and kept on ice in cMRM (250 mM sucrose, 10 mM Hepes, pH 7.4, 0.8 mM ADP, 2 mM ATP, and 5 mM sodium succinate). Mitochondria (70 μ g) were incubated with 3 μ L of reticulocyte lysate containing 35 S-labeled proteins for 15 min at 30 °C to perform the import reaction. After the incubation, mitochondria were reisolated by centrifugation at 10,000 \times g for 5 min and subjected to SDS/PAGE. 35 S-labeled proteins were generated using a TNT kit (Promega). ISP and OTC plasmids were expressed in pGEM-3Z. Imported bands were quantified with a phosphorimager (Fujifilm FLA-7000). The recombinant proteins SOD1^{WT}, SOD1^{G93A}, and SOD1^{G85R} were generated

in SF21 cells as previously described (23). α -Synuclein [WT (S7820) and E46K (S4447)] was purchased from Sigma. Additional materials and methods are discussed in *SI Materials and Methods*.

ACKNOWLEDGMENTS. We thank Pak Chan (Stanford University, Palo Alto, CA) for SOD1^{WT} rats, Jason Young (McGill University, Montreal) and W. Neupert (Ludwig-Maximilians University, Munich) for mitochondrial protein import plasmids, and Larry Hayward (University of Massachusetts Medical School, Worcester, MA) for SOD1 baculovirus stock. This work was supported by National Institutes of Health Grant NS 27036 (to D.W.C.), the Washington University McDonnell Center for Cellular and Molecular Neurobiology, the classmates of Chris Hobler, and the Hope Center for Neurological Disorders at the Washington University (T.M.M.). T.M.M. and C.V.V. were supported at the University of California at San Diego by a K12 award from the National Institute on Aging (AG000975) and by a Muscular Dystrophy Association Development grant, respectively.

- Boillée S, Vande Velde C, Cleveland DW (2006) ALS: A disease of motor neurons and their nonneuronal neighbors. *Neuron* 52:39–59.
- Brujin LI, Miller TM, Cleveland DW (2004) Unraveling the mechanisms involved in motor neuron degeneration in ALS. *Annu Rev Neurosci* 27:723–749.
- Boillée S, et al. (2006) Onset and progression in inherited ALS determined by motor neurons and microglia. *Science* 312:1389–1392.
- Rothstein JD (2009) Current hypotheses for the underlying biology of amyotrophic lateral sclerosis. *Ann Neurol* 65(Suppl 1):S3–S9.
- Ilieva H, Polymenidou M, Cleveland DW (2009) Non-cell autonomous toxicity in neurodegenerative disorders: ALS and beyond. *J Cell Biol* 187:761–772.
- Wang L, et al. (2008) Restricted expression of mutant SOD1 in spinal motor neurons and interneurons induces motor neuron pathology. *Neurobiol Dis* 29:400–408.
- Yamanaka K, et al. (2008) Mutant SOD1 in cell types other than motor neurons and oligodendrocytes accelerates onset of disease in ALS mice. *Proc Natl Acad Sci USA* 105:7594–7599.
- Yamanaka K, et al. (2008) Astrocytes as determinants of disease progression in inherited amyotrophic lateral sclerosis. *Nat Neurosci* 11:251–253.
- Beers DR, et al. (2006) Wild-type microglia extend survival in PU.1 knockout mice with familial amyotrophic lateral sclerosis. *Proc Natl Acad Sci USA* 103:16021–16026.
- Wallace DC (2005) A mitochondrial paradigm of metabolic and degenerative diseases, aging, and cancer: A dawn for evolutionary medicine. *Annu Rev Genet* 39:359–407.
- Damiano M, et al. (2006) Neural mitochondrial Ca²⁺ capacity impairment precedes the onset of motor symptoms in G93A Cu/Zn-superoxide dismutase mutant mice. *J Neurochem* 96:1349–1361.
- Hervias I, Beal MF, Manfredi G (2006) Mitochondrial dysfunction and amyotrophic lateral sclerosis. *Muscle Nerve* 33:598–608.
- Reyes NA, et al. (2010) Blocking the mitochondrial apoptotic pathway preserves motor neuron viability and function in a mouse model of amyotrophic lateral sclerosis. *J Clin Invest* 120:3673–3679.
- Pedrinì S, et al. (2010) ALS-linked mutant SOD1 damages mitochondria by promoting conformational changes in Bcl-2. *Hum Mol Genet* 19:2974–2986.
- Hirano A, Donnenfeld H, Sasaki S, Nakano I (1984) Fine structural observations of neurofilamentous changes in amyotrophic lateral sclerosis. *J Neuropathol Exp Neurol* 43:461–470.
- Sasaki S, Iwata M (2007) Mitochondrial alterations in the spinal cord of patients with sporadic amyotrophic lateral sclerosis. *J Neuropathol Exp Neurol* 66:10–16.
- Okado-Matsumoto A, Fridovich I (2001) Subcellular distribution of superoxide dismutases (SOD) in rat liver: Cu,Zn-SOD in mitochondria. *J Biol Chem* 276:38388–38393.
- Field LS, Furukawa Y, O'Halloran TV, Culotta VC (2003) Factors controlling the uptake of yeast copper/zinc superoxide dismutase into mitochondria. *J Biol Chem* 278:28052–28059.
- Sturtz LA, Diekert K, Jensen LT, Lill R, Culotta VC (2001) A fraction of yeast Cu,Zn-superoxide dismutase and its metallochaperone, CCS, localize to the intermembrane space of mitochondria. A physiological role for SOD1 in guarding against mitochondrial oxidative damage. *J Biol Chem* 276:38084–38089.
- Liu J, et al. (2004) Toxicity of familial ALS-linked SOD1 mutants from selective recruitment to spinal mitochondria. *Neuron* 43:5–17.
- Vande Velde C, Miller TM, Cashman NR, Cleveland DW (2008) Selective association of misfolded ALS-linked mutant SOD1 with the cytoplasmic face of mitochondria. *Proc Natl Acad Sci USA* 105:4022–4027.
- Bergemalm D, et al. (2006) Overloading of stable and exclusion of unstable human superoxide dismutase-1 variants in mitochondria of murine amyotrophic lateral sclerosis models. *J Neurosci* 26:4147–4154.
- Israelson A, et al. (2010) Misfolded mutant SOD1 directly inhibits VDAC1 conductance in a mouse model of inherited ALS. *Neuron* 67:575–587.
- Lukas TJ, Luo WW, Mao H, Cole N, Siddique T (2006) Informatics-assisted protein profiling in a transgenic mouse model of amyotrophic lateral sclerosis. *Mol Cell Proteomics* 5:1233–1244.
- Bergemalm D, et al. (2009) Changes in the spinal cord proteome of an amyotrophic lateral sclerosis murine model determined by differential in-gel electrophoresis. *Mol Cell Proteomics* 8:1306–1317.
- Fukada K, Zhang F, Vien A, Cashman NR, Zhu H (2004) Mitochondrial proteomic analysis of a cell line model of familial amyotrophic lateral sclerosis. *Mol Cell Proteomics* 3:1211–1223.
- Link AJ, et al. (1999) Direct analysis of protein complexes using mass spectrometry. *Nat Biotechnol* 17:676–682.
- Pun S, Santos AF, Saxena S, Xu L, Caroni P (2006) Selective vulnerability and pruning of phasic motoneuron axons in motoneuron disease alleviated by CNTF. *Nat Neurosci* 9:408–419.
- Zybailov B, et al. (2006) Statistical analysis of membrane proteome expression changes in *Saccharomyces cerevisiae*. *J Proteome Res* 5:2339–2347.
- Bailey AO, et al. (2007) RCADiA: Simple automation platform for comparative multidimensional protein identification technology. *Anal Chem* 79:6410–6418.
- Bukau B, Horwich AL (1998) The Hsp70 and Hsp60 chaperone machines. *Cell* 92:351–366.
- Schilling B, et al. (2005) Rapid purification and mass spectrometric characterization of mitochondrial NADH dehydrogenase (complex I) from rodent brain and a dopaminergic neuronal cell line. *Mol Cell Proteomics* 4:84–96.
- Murray J, et al. (2003) The subunit composition of the human NADH dehydrogenase obtained by rapid one-step immunopurification. *J Biol Chem* 278:13619–13622.
- Willis JH, et al. (2009) Isolated deficiencies of OXPHOS complexes I and IV are identified accurately and quickly by simple enzyme activity immunocapture assays. *Biochim Biophys Acta* 1787:533–538.
- Graf L, Lingelbach K, Hoogenraad J, Hoogenraad N (1988) Mitochondrial import of rat pre-ornithine transcarbamylase: Accurate processing of the precursor form is not required for uptake into mitochondria, nor assembly into catalytically active enzyme. *Protein Eng* 2:297–300.
- Söllner T, Griffiths G, Pfaller R, Pfanner N, Neupert W (1989) MOM19, an import receptor for mitochondrial precursor proteins. *Cell* 59:1061–1070.
- Neupert W, Brunner M (2002) The protein import motor of mitochondria. *Nat Rev Mol Cell Biol* 3:555–565.
- Kirkinezos IG, et al. (2005) Cytochrome c association with the inner mitochondrial membrane is impaired in the CNS of G93A-SOD1 mice. *J Neurosci* 25:164–172.
- Pandey N, Schmidt RE, Galvin JE (2006) The alpha-synuclein mutation E46K promotes aggregation in cultured cells. *Exp Neurol* 197:515–520.
- Zarranz JJ, et al. (2004) The new mutation, E46K, of alpha-synuclein causes Parkinson and Lewy body dementia. *Ann Neurol* 55:164–173.
- Banerjee K, et al. (2010) Alpha-synuclein induced membrane depolarization and loss of phosphorylation capacity of isolated rat brain mitochondria: Implications in Parkinson's disease. *FEBS Lett* 584:1571–1576.
- Cappello F, Tripodo C, Farina F, Franco V, Zummo G (2004) HSP10 selective preference for myeloid and megakaryocytic precursors in normal human bone marrow. *Eur J Histochem* 48:261–265.
- Cappello F, Rappa F, David S, Anzalone R, Zummo G (2003) Immunohistochemical evaluation of PCNA, p53, HSP60, HSP10 and MUC-2 presence and expression in prostate carcinogenesis. *Anticancer Res* 23(2B):1325–1331.
- Mattiazzi M, et al. (2002) Mutated human SOD1 causes dysfunction of oxidative phosphorylation in mitochondria of transgenic mice. *J Biol Chem* 277:29626–29633.
- Kushnareva Y, Murphy AN, Andreyev A (2002) Complex I-mediated reactive oxygen species generation: Modulation by cytochrome c and NAD(P)⁺ oxidation-reduction state. *Biochem J* 368:545–553.
- Rosignol R, Malgat M, Mazat JP, Letellier T (1999) Threshold effect and tissue specificity. Implication for mitochondrial cytopathies. *J Biol Chem* 274:33426–33432.
- Mootha VK, et al. (2003) Integrated analysis of protein composition, tissue diversity, and gene regulation in mouse mitochondria. *Cell* 115:629–640.
- Taylor SW, et al. (2003) Characterization of the human heart mitochondrial proteome. *Nat Biotechnol* 21:281–286.
- Sickmann A, et al. (2003) The proteome of *Saccharomyces cerevisiae* mitochondria. *Proc Natl Acad Sci USA* 100:13207–13212.
- Roesch K, Curran SP, Tranebjærg L, Koehler CM (2002) Human deafness dystonia syndrome is caused by a defect in assembly of the DDP1/TIMM8a-TIMM13 complex. *Hum Mol Genet* 11:477–486.
- Bekris LM, et al. (2008) Multiple SNPs within and surrounding the apolipoprotein E gene influence cerebrospinal fluid apolipoprotein E protein levels. *J Alzheimers Dis* 13:255–266.
- Takei N, et al.; Japanese Genetic Study Consortium for Alzheimer Disease (2009) Genetic association study on and around the APOE in late-onset Alzheimer disease in Japanese. *Genomics* 93:441–448.
- Devi L, Prabhu BM, Galati DF, Avadhani NG, Anandatheerthavarada HK (2006) Accumulation of amyloid precursor protein in the mitochondrial import channels of human Alzheimer's disease brain is associated with mitochondrial dysfunction. *J Neurosci* 26:9057–9068.